Adsorption 8: 111–123, 2002

# Thermodynamic Description of Excess Isotherms in High-Pressure Adsorption of Methane, Argon and Nitrogen

ALEXANDER HERBST AND PETER HARTING
*Institute of Non-Classical Chemistry at the University of Leipzig, Permoserstr, 15 D-4318 Leipzig, Germany*
herbst@inc.uni.leipzig.de
harting@inc.uni-leipzig.de
http://www.uni-leipzig.de/~inc

*Received January 26, 2001; Revised February 26, 2002; Accepted February 27, 2002*

**Abstract.** In the present work the supercritical fluids argon, methane and nitrogen were picked out as examples, and the results of analysis concerning the adsorption of these fluids at activated carbon Norit R1 (Norit company, Germany) and SCS-3 (ISPE, Kiev) at different temperatures up to a pressure of 50 MPa are presented and discussed in this paper. The principle of working of the measuring device is described in this context as well.

A three-parameter isothermal equation is used to represent the adsorption equilibrium. The isothermal equation is based on a physical model concept which has already been used for the modelling of adsorption processes with a pressure up to 15 MPa.

**Keywords:** excess adsorption, high pressure, gravimetric measurement, supercritical fluids, activated carbon

## Introduction

Physical adsorption of fluids onto solids is of interest in the transportation and storage of fuel and radioactive gases, the separation and cleaning of materials, solid-phase extractions, adsorbent regenerations using supercritical fluids, supercritical fluid chromatography and critical-point drying. Although physical adsorption of pure gases on different porous solids has been extensively studied over a wide range of temperatures and pressures, the number of works related to adsorption at high pressures is limited.

In adsorption experiments the excess adsorption only can be measured, which is defined as the excess gas present in the pores and on the surface of the adsorbent and above it corresponding to the density of the gas in the bulk phase at the given temperature and pressure.

The aims of this research work are the measurement and the thermodynamic description of the excess in the adsorption of gases up to pressures of 50 MPa. Different adsorbents were tested to determine for example the influence of the structure of pores under high pressure to obtain specific characteristics of these materials.

## Characterization of Adsorbents

Two different adsorbents were tested: activated carbon Norit R1 (Norit company, Germany) and activated carbon SCS-3 from the Institute of Sorption and Problems of Endoecology (Ukraine). Both adsorbents were exposed to high pressure up to 50 MPa during the adsorption process.

To compare both adsorbents the surfaces of them were firstly recorded by a digital scanning electron microscope DSM 940 (Zeiss company, Germany) in different enlargements (Fig. 1). Secondly, the adsorbents were analyzed by nitrogen adsorption at 77 K using ASAP-2000M (Micromeritics company, USA). Nitrogen adsorption was needed to determine the

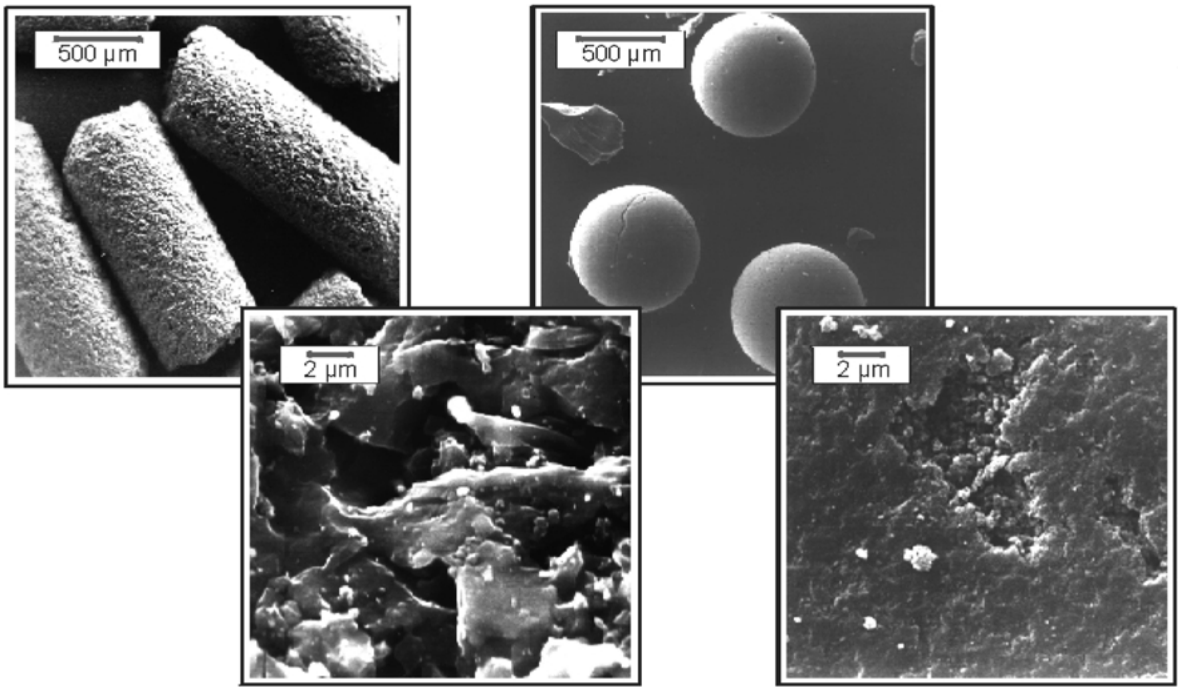

*Figure 1.* Pictures of the adsorbent Norit R1 (left) and SCS-3 (right).

specific areas and the specific pore volume of the adsorbent studied by using the following methods: the classical BET equation and its extended form to n-layers, the t-plot method and the density functional theory (DFT). The resulting data are summarized in Table 1.

The BET surface areas 1339 and 1094 m$^2$/g, the micro-pore volumes 0.6446 and 0.4382 cm$^3$/g, and the total pore volumes 0.7074 and 1.0534 cm$^3$/g were obtained for the conventional activated carbon Norit R1 and the synthetic carbon SCS-3 (sterene-divinylbenzene copolymer), respectively.

## Experiment

High pressure adsorption measurements were performed on a magnetic suspension balance, Rubotherm (Bochum, Germany). The balance working up to 50 MPa, allows the determination of specific quantities, e.g. solubility of substances in fluids, density of fluids and adsorption behaviour of fluids on adsorbents even in corrosive media without danger of pollution or destruction of the balance. In comparison to traditional balances the test substance is not directly connected with the balance, it hangs on a so-called suspension magnet. The weight to measure is transmitted by magnetic suspension coupling from a closed and pressure-proof metal container to an external microbalance. The suspension consists of a measuring load, a sensor core and a permanent magnet (Fig. 2). Regulation systems keep the electric magnet in free suspension and transmit the weight to measure to the external balance.

*Table 1.* Properties of adsorbents.

| | Norit R1 | SCS-3 |
|---|---|---|
| BET surface (m$^2$/g) | 1339 | 1094 |
| Internal surface (t-plot) (m$^2$/g) | 1307 | 929 |
| Volume of micro-pores (cm$^3$/g) | 0.6446 | 0.4382 |
| Total volume (cm$^3$/g) | 0.7074 | 1.0534 |

The measuring cell consists of a conventional high-pressure stainless steel sample cell, which was connected to a gas reservoir via an air driven gas booster (Haskel, USA). The gases used were ultra-high purity grade supplied by Air Liquid. A known amount of active carbon (∼4 g), which was outgassed at 423 K, was placed into the sample pan of the balance. Before the measurements the system was evacuated at $2 \times 10^{-3}$ hPa. Equilibrium weights were achieved in 20–30 min.

*Table 2.* Systems already measured.

| Adsorbent | 25°C | 40°C | 55°C | 70°C |
|---|---|---|---|---|
| Norit R1 | He, $CH_4$, Ar, $N_2$ | $CH_4$, Ar, $N_2$ | He, $CH_4$, Ar, $N_2$ | He, $CH_4$, Ar, $N_2$ |
| SCS-3 | $CH_4$, Ar, $N_2$ | $CH_4$, Ar, $N_2$ | | |

The measurements of excess adsorption isotherms of the pure gases methane, argon and nitrogen on the both adsorbents were carried out at four temperatures from 298, 313, 328 and 343 K over a wide pressure range from 0 to 50 MPa (Table 2). These adsorption isotherms are typical excess isotherms with a distinct maximum.

The originally measured $m^{\mathrm{s}}$ values of the balance for all gases are presented in the Appendix in Tables 7–19.

### *Analysis of Row Gravimetric Adsorption Measurement Data*

Row gravimetric adsorption measurement data $m^{\mathrm{s}}$ include also quantities concerning experimental equipment, for example the container which contains the sample. The parameter $V_{\mathrm{cont}}$ represent the volume of the container. It can be determined separately by buoyancy measurements with the empty balance and with the sample container without adsorbents. The resulting values for all measured systems are summarized in Table 3. First the row data must corrected by the equipment quantities to come to equipment independent data, to the so-called reduced mass $\Omega$ in the sense of Staudt et al. (1993).

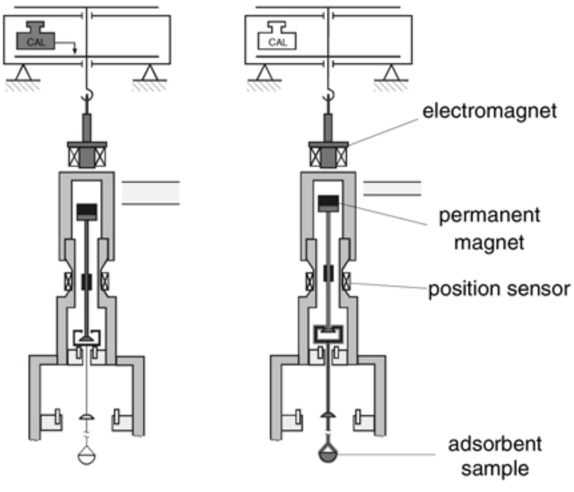

*Figure 2.* Operating principle of magnetic suspension balance.

*Table 3.* Mass of adsorbent and the measured values for $V_{\mathrm{cont}}$ and $\bar{V}_{\mathrm{ads,He}}$.

| | 298 K | 313 K | 328 K | 343 K | $V_{\mathrm{cont}}$ (cm$^3$) |
|---|---|---|---|---|---|
| $m$ (g), Nitrogen | 4.08325 | | 4.12680 | 4.14252 | 0.70492 |
| $m$ (g), Argon | 4.08325 | | | 4.14252 | 0.70492 |
| $m$ (g), Methane | 4.37217 | | | | 1.97883 |
| $\bar{V}_{\mathrm{ads,He}}$ (cm$^3$/g) | 0.46161 | 0.46898 | 0.47335 | 0.47768 | |

$$\Omega = m^{\mathrm{s}} + \rho_{\mathrm{fluid}} \cdot V_{\mathrm{cont}} \tag{1}$$

With the gravimetric adsorption measurements only the sum of excess $\Gamma$ and buoyancy $\rho_{\mathrm{fluid}} V_{\mathrm{ads}}$ can be obtained (Staudt et al., 1993; Talu, 1998). The results for the specific excess $\bar{\Gamma}$ are as follows:

$$\bar{\Gamma} = \frac{\Omega + \rho_{\mathrm{fluid}} \cdot V_{\mathrm{ads}}}{m} \tag{2}$$

with $\bar{\Gamma}$ is specific excess adsorption, $\rho_{\mathrm{fluid}}$ is density of the fluid, $V_{\mathrm{ads}}$ is volume of the empty adsorbent, and $m$ mass of adsorbent at microbalance.

The skeletal volume of the adsorbent $V_{\mathrm{ads}}$ can be determined by means of buoyancy measurements with helium as fluid (Sircar, 1999; Staudt et al., 1993; Talu, 1998). It is based on the assumption that helium is not adsorbed ($\Gamma = 0$) but fills out the pore volume without changing the pore structure of the adsorbent. The resulting, so called helium volume of porous solids $V_{\mathrm{ads,He}}$ can be calculated from the microbalance signal $m^{\mathrm{s}}$ and knowing $V_{\mathrm{cont}}$ as

$$V_{\mathrm{ads,He}} = \frac{-(\rho_{\mathrm{He}} \cdot V_{\mathrm{cont}} + m^{\mathrm{s}})}{\rho_{\mathrm{He}}} \tag{3}$$

### *Helium on Activated Carbon Norit R1*

The skeletal volume of the adsorbent can be determined by means of buoyancy measurements with helium as fluid (Neimark and Ravikovich, 1997; Staudt et al.; Malbrunot et al., 1997; Vazquez et al., 1987). The values of the volume of the adsorbent in Fig. 3 were calculated for each experimental point at pressure $p$. Assuming Helium not be adsorbed and only buoyancy occur, the buoyancy related volume of adsorbent can be calculated using the experimental point at pressure $p$ and vacuum ($p = 0$).

$$V_{\mathrm{ads}}(p) = -\frac{\Omega(p) - \Omega(p = 0)}{\rho_{\mathrm{He}}(p) - \rho_{\mathrm{He}}(p = 0)}$$

The experimental determination of the volume of the activated carbons by means of this method shows at low pressures a decrease of the volume. At a certain pressure the volume increase again with increasing pressure (see in Fig. 3 by example of Norit R1). This behavior can be explained by the pressure dependence of the volume of porous solids. First, with increasing pressure the adsorbent will be compressed by the surrounding fluid. The increase of the volume is caused by penetration of helium in to the adsorbent combined with swelling of the crystal structure. Additionally, a temperature dependence can be observed here.

The classical method for determination of the volume of adsorbent is described in Staudt et al., Staudt et al. (1993), and Talu (1998). The results using this method are shown in Fig. 4, where the specific mass of the sample of adsorbent at the microbalance were plotted in dependence of the density of fluid (Sircar, 1999; Malbrunot et al., 1992). The slop of this isotherm is volume $\bar{V}_{\mathrm{ads,He}}$. On the basis of the temperature dependence of volume of adsorbent, $\bar{V}_{\mathrm{ads,He}}$ were determined

*Table 4*. Thermodynamic quantities $I_0, k_0, v_0$ and $\bar{V}_{\mathrm{ads}}$ for the different temperatures by measurements on SCS-3.

| Gas | $T$ (K) | $I_0$ (mg/g) | $k_0$ (MPa) | $v_0$ (cm$^3$/mol) | $\bar{V}_{\mathrm{ads}}$ (cm$^3$/g) |
|---|---|---|---|---|---|
| Nitrogen | 298.15 | 172.23 | 2.003 | 280.23 | 0.36 |
| | 313.15 | 184.83 | 2.741 | 267.32 | 0.36 |
| Argon | 298.15 | 360.77 | 3.412 | 242.94 | 0.35 |
| | 313.15 | 361.04 | 4.504 | 225.33 | 0.36 |
| Methane | 298.15 | 121.75 | 1.135 | 379.74 | 0.33 |
| | 313.15 | 157.71 | 1.698 | 356.18 | 0.32 |

*Table 5*. Thermodynamic quantities $I_0, k_0, v_0$ and $\bar{V}_{\mathrm{ads}}$ for the different temperatures by measurements on Norit R1.

| Gas | $T$ (K) | $I_0$ (mg/g) | $k_0$ (MPa) | $v_0$ (cm$^3$/mol) | $\bar{V}_{\mathrm{ads}}$ (cm$^3$/g) |
|---|---|---|---|---|---|
| Nitrogen | 298.15 | 190.41 | 2.03 | 292.49 | 0.29 |
| | 313.15 | 192.93 | 2.76 | 282.27 | 0.30 |
| | 328.15 | 196.05 | 3.66 | 272.02 | 0.31 |
| | 343.15 | 197.64 | 4.86 | 259.98 | 0.31 |
| Argon | 298.15 | 454.97 | 4.24 | 228.93 | 0.33 |
| | 313.15 | 452.24 | 5.33 | 221.61 | 0.34 |
| | 328.15 | 474.06 | 7.50 | 207.33 | 0.35 |
| | 343.15 | 463.09 | 9.14 | 197.93 | 0.36 |
| Methane | 298.15 | 144.45 | 0.95 | 414.23 | 0.27 |
| | 313.15 | 147.01 | 1.42 | 380.07 | 0.27 |
| | 328.15 | 140.97 | 1.74 | 353.92 | 0.30 |
| | 343.15 | 140.67 | 2.22 | 330.03 | 0.31 |

*Table 6*. Adsorption heats of the gases methane, argon and nitrogen on Norit R1.

| Gas | Methane | Argon | Nitrogen |
|---|---|---|---|
| $q$ (kJ/mol) | −15.81 | −15.22 | −16.64 |

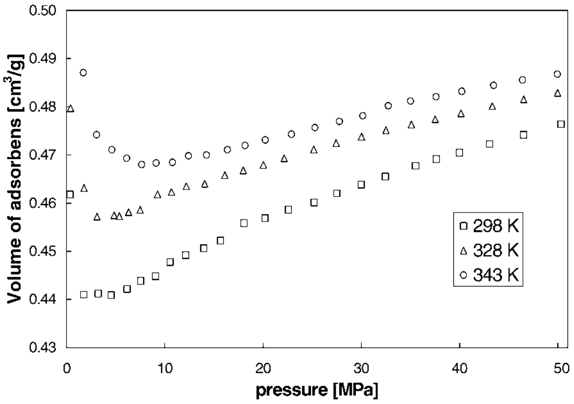

*Figure 3*. Measurements of the buoyancy with helium on activated carbon Norit R1 at 298, 328 and 343 K.

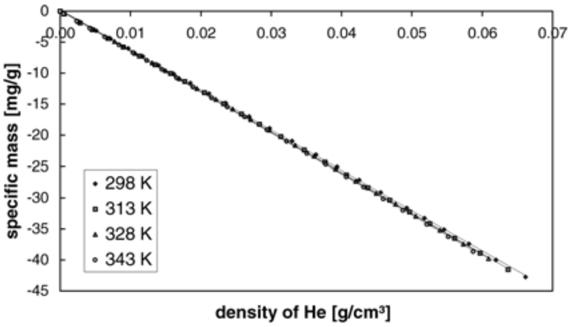

*Figure 4*. Determination of helium-volume of Norit R1 at 298, 313, 328 and 343 K.

for all measurement temperatures (Fig. 4). With increasing temperature an increase of the volume of porous solids can be observed (see Table 3).

## The Three-Parameter Isothermal Equation

The thermodynamic description of the excess is possible with the following three-parameter isothermal equation of the form:

$$\bar{\Gamma}(p,T) = \frac{f}{f + k_0 \exp\left(\frac{v_0 \cdot p}{R \cdot T}\right)} \cdot I_0 \qquad (4)$$

with $I_0$ is maximal loading (mg/g), $k_0$ is Henry-constant (MPa), $v_0$ is molar volume (cm$^3$/mol), $f$ is fugacity (MPa), $p$ is pressure (MPa), $R$ gas constant (cm$^3 * $MPa/mol $*$ K), and $T$ is temperature (K).

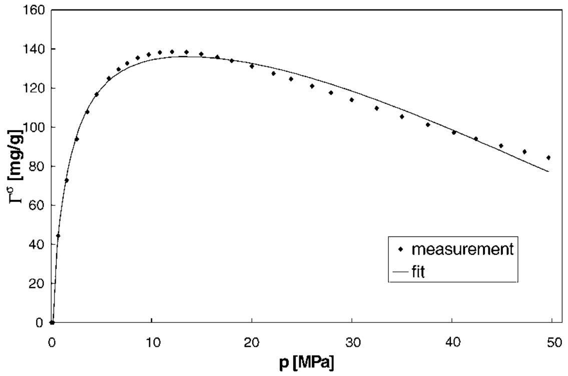

*Figure 5.* The first modelling of the excess adsorption of nitrogen on Norit R1 at 298 K.

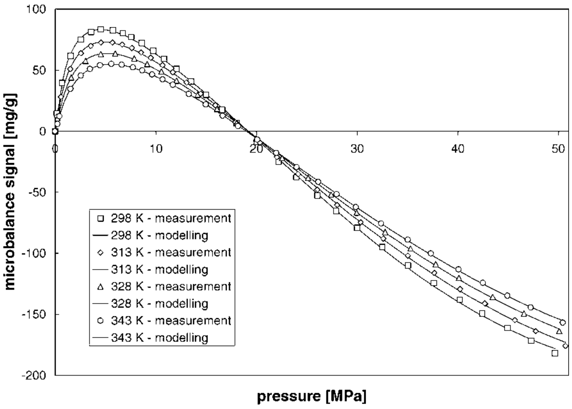

*Figure 6.* Modellings of the measured values of nitrogen on Norit R1 at 298, 313, 328 and 343 K.

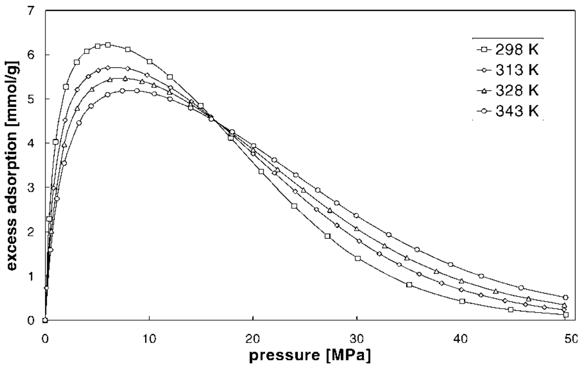

*Figure 7.* Calculated adsorption excess of methane on Norit R1 at 298, 313, 328 and 343 K.

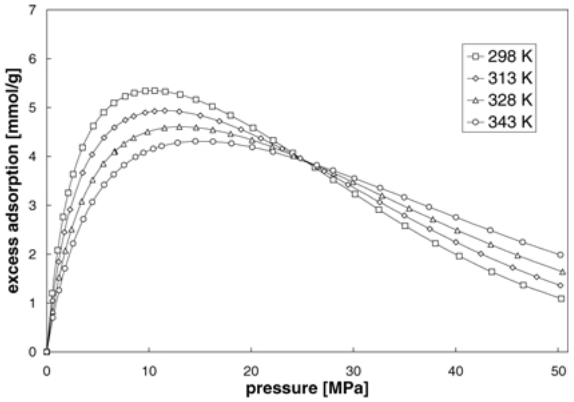

*Figure 8.* Calculated adsorption excess of argon on Norit R1 at 298, 313, 328 and 343 K.

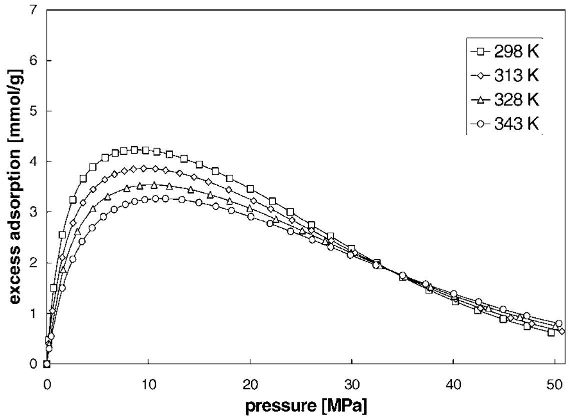

*Figure 9.* Calculated adsorption excess of nitrogen on Norit R1 at 298, 313, 328 and 343 K.

*Table 7.* Measurements of the buoyancy with helium on activated carbon Norit R1 at 298, 328 and 343 K.

| 298 K | | | 328 K | | | 343 K | | |
|---|---|---|---|---|---|---|---|---|
| $p$ (MPa) | $m^s$ (mg) | $\bar{\Omega}$ (mg/g) | $p$ (MPa) | $m^s$ (mg) | $\bar{\Omega}$ (mg/g) | $p$ (MPa) | $m^s$ (mg) | $\bar{\Omega}$ (mg/g) |
| 0.000 | 0.00 | 0.00 | 0.000 | 0.00 | 0.00 | 0.000 | 0.00 | 0.00 |
| 0.350 | −1.49 | −0.36 | 0.410 | −1.63 | −0.39 | 0.380 | −1.66 | −0.40 |
| 1.750 | −7.16 | −1.73 | 1.770 | −6.82 | −1.65 | 1.710 | −6.54 | −1.58 |
| 3.221 | −13.09 | −3.17 | 3.101 | −11.77 | −2.85 | 3.051 | −11.38 | −2.76 |
| 4.531 | −18.29 | −4.43 | 4.831 | −18.21 | −4.41 | 4.631 | −17.08 | −4.14 |
| 6.161 | −24.73 | −5.99 | 5.381 | −20.23 | −4.90 | 6.121 | −22.38 | −5.42 |
| 7.542 | −30.16 | −7.31 | 6.321 | −23.70 | −5.74 | 7.632 | −27.68 | −6.71 |
| 9.062 | −36.04 | −8.73 | 7.491 | −27.97 | −6.78 | 9.112 | −32.87 | −7.96 |
| 10.532 | −41.80 | −10.13 | 9.262 | −34.50 | −8.36 | 10.792 | −38.68 | −9.37 |
| 12.122 | −47.87 | −11.60 | 10.672 | −39.55 | −9.58 | 12.422 | −44.33 | −10.74 |
| 13.983 | −54.88 | −13.29 | 12.182 | −44.95 | −10.89 | 14.263 | −50.55 | −12.25 |
| 15.673 | −61.20 | −14.83 | 14.053 | −51.50 | −12.48 | 16.373 | −57.65 | −13.97 |
| 18.054 | −70.15 | −16.99 | 16.123 | −58.75 | −14.23 | 18.174 | −63.64 | −15.42 |
| 20.194 | −77.85 | −18.86 | 17.974 | −65.11 | −15.77 | 20.214 | −70.36 | −17.05 |
| 22.585 | −86.40 | −20.93 | 20.024 | −72.07 | −17.46 | 22.905 | −79.06 | −19.15 |
| 25.185 | −95.49 | −23.13 | 22.144 | −79.20 | −19.19 | 25.265 | −86.62 | −20.98 |
| 27.506 | −103.57 | −25.09 | 25.165 | −89.19 | −21.61 | 27.786 | −94.56 | −22.91 |
| 29.986 | −112.04 | −27.14 | 27.435 | −96.58 | −23.40 | 30.146 | −101.89 | −24.68 |
| 32.436 | −120.27 | −29.14 | 30.016 | −104.83 | −25.40 | 32.747 | −109.98 | −26.64 |
| 35.527 | −130.50 | −31.61 | 32.517 | −112.72 | −27.31 | 35.007 | −116.79 | −28.29 |
| 37.638 | −137.35 | −33.27 | 35.097 | −120.71 | −29.24 | 37.608 | −124.47 | −30.15 |
| 39.988 | −144.84 | −35.09 | 37.528 | −128.11 | −31.04 | 40.228 | −132.13 | −32.01 |
| 43.069 | −154.50 | −37.43 | 40.158 | −136.00 | −32.95 | 43.469 | −141.43 | −34.26 |
| 46.499 | −165.04 | −39.98 | 43.349 | −145.44 | −35.23 | 46.429 | −149.76 | −36.28 |
| 50.320 | −176.54 | −42.77 | 46.519 | −154.62 | −37.46 | 49.950 | −159.47 | −38.63 |
| | | | 49.980 | −164.40 | −39.83 | | | |

The equation was derived with a physical model based on the equality of the chemical potentials of the adsorbed and the fluid phase (Harting et al.). Until now this equation was applied for pressures up to about 15 MPa (Salem, 1997). However, the first applications of the three-parameter isothermal equation on the gases methane, argon and nitrogen over the entire pressure range of up to 50 MPa showed significant deviation values (see Fig. 5 by the example of nitrogen at 298 K). These deviations become still larger in the cases of methane and argon. This was caused primarily by the necessary buoyancy correction, which was carried out with helium as reference gas. Therefore, this aspect requires more attention.

## Extension of the Three-Parameter Isothermal Equation

The Eq. (5) results from Eqs. (1), (2) and (4). Equation (5) allows the modelling of the specific reduced (equipment independent) mass $\bar{\Omega}$ with $\bar{V}_{\text{ads}}$ as an additional fitting parameter:

$$\bar{\Omega} = \frac{f}{f + k_0 \exp\left(\frac{v_0 \cdot p}{R \cdot T}\right)} \cdot I_0 - \rho_{\text{fluid}} \cdot \bar{V}_{\text{ads}} \qquad (5)$$

with $\bar{\Omega}$ is specific reduced mass and $\bar{V}_{\text{ads}}$ is specific volume of the adsorbent.

Therefore, it is proposed to use the precisely measured values of adsorption for the thermodynamic modelling without additional information (volume of

*Table 8.* Measurements with nitrogen on activated carbon Norit R1 at 298 K.

| $p$ (MPa) | $\rho_{\text{fluid}}$ (g/cm$^3$) | $m^s$ (mg) | $\bar{\Omega}$ (mg/g) | $\bar{\Gamma}_{\text{He}}$ (mg/g) | $\bar{\Gamma}_{3-\text{PIG}}$ (mg/g) |
|---|---|---|---|---|---|
| 0.000 | 0.00000 | 0.00 | 0.000 | 0.000 | 0.000 |
| 0.170 | 0.00192 | 60.74 | 15.207 | 16.094 | 14.453 |
| 0.670 | 0.00758 | 161.09 | 40.760 | 44.259 | 44.498 |
| 1.530 | 0.01733 | 251.60 | 64.609 | 72.607 | 73.484 |
| 2.541 | 0.02879 | 306.49 | 80.031 | 93.320 | 91.495 |
| 3.581 | 0.04060 | 332.36 | 88.405 | 107.146 | 101.926 |
| 4.511 | 0.05115 | 340.94 | 92.328 | 115.941 | 107.597 |
| 5.731 | 0.06497 | 337.94 | 93.979 | 123.969 | 111.995 |
| 6.711 | 0.07603 | 327.89 | 93.426 | 128.520 | 113.915 |
| 7.562 | 0.08558 | 315.10 | 91.943 | 131.445 | 114.770 |
| 8.612 | 0.09730 | 294.93 | 89.028 | 133.943 | 115.046 |
| 9.722 | 0.10960 | 269.60 | 84.947 | 135.539 | 114.609 |
| 10.822 | 0.12166 | 241.81 | 80.223 | 136.382 | 113.593 |
| 12.052 | 0.13498 | 208.22 | 74.296 | 136.601 | 111.905 |
| 13.493 | 0.15030 | 166.67 | 66.765 | 136.142 | 109.321 |
| 14.983 | 0.16581 | 121.85 | 58.466 | 135.002 | 106.083 |
| 16.583 | 0.18203 | 72.36 | 49.146 | 133.169 | 102.083 |
| 18.014 | 0.19611 | 27.75 | 40.652 | 131.178 | 98.131 |
| 20.034 | 0.21531 | −35.20 | 28.550 | 127.937 | 92.071 |
| 22.194 | 0.23489 | −102.02 | 15.566 | 123.993 | 85.137 |
| 23.945 | 0.25003 | −153.95 | 5.463 | 120.879 | 79.303 |
| 26.045 | 0.26735 | −214.78 | −6.445 | 116.965 | 72.188 |
| 27.916 | 0.28201 | −266.98 | −16.698 | 113.479 | 65.867 |
| 29.986 | 0.29744 | −322.83 | −27.714 | 109.583 | 59.009 |
| 32.486 | 0.31499 | −387.00 | −40.398 | 105.002 | 51.085 |
| 35.027 | 0.33171 | −448.68 | −52.617 | 100.501 | 43.593 |
| 37.608 | 0.34763 | −507.83 | −64.355 | 96.112 | 36.682 |
| 40.188 | 0.36257 | −563.60 | −75.434 | 91.930 | 30.541 |
| 42.408 | 0.37471 | −609.12 | −84.486 | 88.481 | 25.890 |
| 44.919 | 0.38770 | −657.81 | −94.167 | 84.797 | 21.316 |
| 47.259 | 0.39918 | −700.82 | −102.720 | 81.539 | 17.670 |
| 49.640 | 0.41026 | −742.41 | −110.992 | 78.385 | 14.520 |

*Table 9.* Measurements with nitrogen on activated carbon Norit R1 at 313 K.

| $p$ (MPa) | $\rho_{\text{fluid}}$ (g/cm$^3$) | $m^s$ (mg) | $\bar{\Omega}$ (mg/g) | $\bar{\Gamma}_{\text{He}}$ (mg/g) | $\bar{\Gamma}_{3-\text{PIG}}$ (mg/g) |
|---|---|---|---|---|---|
| 0.000 | 0.00000 | 0.00 | 0.000 | 0.000 | 0.0000 |
| 0.190 | 0.00204 | 49.72 | 12.530 | 13.489 | 12.1817 |
| 0.570 | 0.00614 | 115.11 | 29.250 | 32.127 | 31.3468 |
| 1.510 | 0.01626 | 208.30 | 53.820 | 61.443 | 61.1465 |
| 2.571 | 0.02766 | 261.04 | 68.705 | 81.678 | 79.6978 |
| 3.551 | 0.03819 | 285.73 | 76.570 | 94.482 | 89.9909 |
| 4.551 | 0.04892 | 296.48 | 81.053 | 103.994 | 96.7282 |
| 5.701 | 0.06120 | 296.93 | 83.284 | 111.985 | 101.5948 |
| 6.661 | 0.07140 | 290.17 | 83.390 | 116.877 | 104.0927 |
| 7.632 | 0.08165 | 278.37 | 82.270 | 120.565 | 105.5964 |
| 8.542 | 0.09121 | 263.83 | 80.359 | 123.135 | 106.3002 |
| 9.502 | 0.10121 | 245.89 | 77.693 | 125.160 | 106.4609 |
| 10.672 | 0.11329 | 221.11 | 73.708 | 126.836 | 106.0141 |
| 11.692 | 0.12369 | 197.32 | 69.677 | 127.683 | 105.1580 |
| 13.063 | 0.13745 | 163.18 | 63.693 | 128.155 | 103.4545 |
| 14.483 | 0.15145 | 125.58 | 56.901 | 127.929 | 101.1419 |
| 15.903 | 0.16515 | 86.68 | 49.739 | 127.190 | 98.3768 |
| 17.914 | 0.18397 | 30.55 | 39.243 | 125.523 | 93.8457 |
| 20.344 | 0.20580 | −38.38 | 26.129 | 122.644 | 87.6365 |
| 22.034 | 0.22034 | −85.78 | 17.032 | 120.370 | 82.9794 |
| 24.125 | 0.23761 | −143.26 | 5.935 | 117.369 | 76.9702 |
| 26.045 | 0.25276 | −195.02 | −4.125 | 114.414 | 71.3156 |
| 27.996 | 0.26747 | −245.93 | −14.054 | 111.382 | 65.5436 |
| 30.326 | 0.28417 | −304.71 | −25.566 | 107.703 | 58.7352 |
| 32.587 | 0.29950 | −359.28 | −36.283 | 104.178 | 52.3441 |
| 35.027 | 0.31516 | −415.89 | −47.445 | 100.359 | 45.7968 |
| 37.648 | 0.33100 | −473.70 | −58.868 | 96.362 | 39.2801 |
| 40.228 | 0.34568 | −527.66 | −69.548 | 92.570 | 33.4555 |
| 42.719 | 0.35907 | −576.59 | −79.220 | 89.176 | 28.4260 |
| 45.639 | 0.37386 | −631.25 | −90.052 | 85.282 | 23.2723 |
| 47.730 | 0.38390 | −668.36 | −97.407 | 82.636 | 20.0604 |
| 50.680 | 0.39736 | −718.19 | −107.287 | 79.068 | 16.1585 |

the adsorbents). The parameters $I_0$, $k_0$, $v_0$ and $\bar{V}_{\text{ads}}$ of Eq. (5) are fitted to the specific reduced mass measured directly at the microbalance. The fit was successful for methane, argon and nitrogen up to 50 MPa at different temperatures. Modellings for both adsorbents used were made. The results show (by the example of nitrogen on Norit R1, Fig. 6) that the Three-Parameter Isothermal Equation for the description of the adsorption isotherms for both different adsorbents are suitable (Norit R1 is a microporous adsorbent, and SCS-3 indicates a large proportion of meso- and macropores). The results of the modellings of methane, argon and nitrogen are summarized for Norit R1 at four different temperatures in Table 5 and for SCS-3 at two temperatures in Table 4, respectively.

The volume of the adsorbent $\bar{V}_{\text{ads}}$, determined from the respective modelling is, as expected, approximately

*Table 10.* Measurements with nitrogen on activated carbon Norit R1 at 328 K.

| $p$ (MPa) | $\rho_{\text{fluid}}$ (g/cm$^3$) | $m^{\text{s}}$ (mg) | $\bar{\Omega}$ (mg/g) | $\bar{\Gamma}_{\text{He}}$ (mg/g) | $\bar{\Gamma}_{3-\text{PIG}}$ (mg/g) |
|---|---|---|---|---|---|
| 0.000 | 0.00000 | 0.00 | 0.000 | 0.000 | 0.0000 |
| 0.230 | 0.00236 | 45.32 | 11.385 | 12.503 | 11.3590 |
| 1.610 | 0.01652 | 181.36 | 46.768 | 54.587 | 53.5147 |
| 3.021 | 0.03094 | 238.14 | 62.990 | 77.635 | 74.4685 |
| 4.531 | 0.04631 | 261.11 | 71.182 | 93.102 | 86.6106 |
| 5.981 | 0.06097 | 262.63 | 74.054 | 102.913 | 93.1655 |
| 7.872 | 0.07988 | 246.15 | 73.291 | 111.102 | 97.5104 |
| 9.142 | 0.09243 | 227.53 | 70.924 | 114.677 | 98.7349 |
| 10.552 | 0.10620 | 202.15 | 67.125 | 117.394 | 98.9996 |
| 12.062 | 0.12071 | 171.19 | 62.102 | 119.240 | 98.3264 |
| 14.153 | 0.14035 | 123.18 | 53.823 | 120.259 | 96.1831 |
| 16.083 | 0.15798 | 75.62 | 45.309 | 120.088 | 93.2718 |
| 17.984 | 0.17480 | 26.90 | 36.377 | 119.121 | 89.7523 |
| 19.964 | 0.19175 | −24.23 | 26.882 | 117.648 | 85.5630 |
| 22.535 | 0.21281 | −90.78 | 14.354 | 115.089 | 79.5554 |
| 25.135 | 0.23303 | −157.44 | 1.654 | 111.959 | 73.0585 |
| 27.395 | 0.24971 | −213.88 | −9.172 | 109.032 | 67.2405 |
| 29.946 | 0.26758 | −275.19 | −20.977 | 105.681 | 60.6509 |
| 32.777 | 0.28625 | −340.69 | −33.659 | 101.840 | 53.4869 |
| 35.287 | 0.30186 | −396.17 | −44.437 | 98.450 | 47.3993 |
| 37.778 | 0.31651 | −448.76 | −54.679 | 95.141 | 41.7027 |
| 40.088 | 0.32942 | −495.72 | −63.853 | 92.078 | 36.7843 |
| 43.459 | 0.34714 | −560.21 | −76.453 | 87.866 | 30.3018 |
| 46.549 | 0.36233 | −616.10 | −87.400 | 84.113 | 25.1120 |
| 50.050 | 0.37845 | −675.48 | −99.036 | 80.107 | 20.0916 |

identical. This proves the plausibility of the description.

The maximal loading $I_0$, which corresponds to the maximal quantity of adsorbate in the adsorption space, was, as expected, temperature-independent. The comparison of the maximal loading between both the measured activated carbons shows that the value $I_0$ depends directly on the micro-pore volumes of the adsorbents. Especially Norit R1, with a larger micropore volume has the larger $I_0$ for all gases presented. This corresponds to the reality and proves, therefore, the plausibility of the modelling.

The molar volume $v_0$ is a characteristic of the adsorbate phase. It is independent of the type of the adsorbent, which is acknowledged by the results of the fits. Consequently the molar volumes are identical for both adsorbents with the same gas.

*Table 11.* Measurements with nitrogen on activated carbon Norit R1 at 343 K.

| $p$ (MPa) | $\rho_{\text{fluid}}$ (g/cm$^3$) | $m^{\text{s}}$ (mg) | $\bar{\Omega}$ (mg/g) | $\bar{\Gamma}_{\text{He}}$ (mg/g) | $\bar{\Gamma}_{3-\text{PIG}}$ (mg/g) |
|---|---|---|---|---|---|
| 0.000 | 0.00000 | 0.00 | 0.000 | 0.000 | 0.000 |
| 0.230 | 0.00226 | 24.70 | 6.439 | 7.518 | 8.759 |
| 0.440 | 0.00432 | 50.80 | 13.187 | 15.250 | 15.827 |
| 1.530 | 0.01500 | 143.50 | 37.732 | 44.895 | 42.561 |
| 2.571 | 0.02515 | 189.00 | 50.628 | 62.640 | 58.448 |
| 3.481 | 0.03399 | 211.30 | 57.617 | 73.855 | 67.959 |
| 4.461 | 0.04348 | 223.90 | 62.340 | 83.109 | 75.277 |
| 5.581 | 0.05426 | 228.20 | 65.253 | 91.171 | 81.130 |
| 6.631 | 0.06429 | 225.60 | 66.349 | 97.059 | 84.918 |
| 7.742 | 0.07481 | 216.90 | 66.035 | 101.771 | 87.633 |
| 8.662 | 0.08346 | 206.40 | 64.956 | 104.825 | 89.119 |
| 9.642 | 0.09259 | 192.80 | 63.203 | 107.434 | 90.104 |
| 10.692 | 0.10228 | 175.70 | 60.687 | 109.546 | 90.605 |
| 11.702 | 0.11150 | 157.60 | 57.845 | 111.106 | 90.644 |
| 13.283 | 0.12569 | 127.00 | 52.802 | 112.843 | 90.005 |
| 14.963 | 0.14046 | 90.90 | 46.511 | 113.609 | 88.583 |
| 16.643 | 0.15489 | 52.90 | 39.694 | 113.681 | 86.568 |
| 18.164 | 0.16760 | 17.50 | 33.220 | 113.282 | 84.338 |
| 20.084 | 0.18323 | −28.30 | 24.701 | 112.226 | 81.096 |
| 21.974 | 0.19809 | −73.40 | 16.222 | 110.845 | 77.541 |
| 23.995 | 0.21340 | −121.40 | 7.110 | 109.048 | 73.452 |
| 26.125 | 0.22890 | −171.70 | −2.532 | 106.812 | 68.920 |
| 27.956 | 0.24171 | −213.90 | −10.657 | 104.803 | 64.920 |
| 29.876 | 0.25463 | −257.40 | −19.079 | 102.554 | 60.679 |
| 32.396 | 0.27083 | −312.70 | −29.825 | 99.547 | 55.136 |
| 35.017 | 0.28680 | −368.20 | −40.661 | 96.338 | 49.504 |
| 37.307 | 0.30006 | −414.80 | −49.784 | 93.549 | 44.767 |
| 40.058 | 0.31518 | −468.50 | −60.325 | 90.231 | 39.380 |
| 42.498 | 0.32791 | −514.10 | −69.295 | 87.341 | 34.924 |
| 44.919 | 0.33994 | −557.50 | −77.847 | 84.536 | 30.834 |
| 47.239 | 0.35095 | −597.40 | −85.718 | 81.927 | 27.234 |
| 50.410 | 0.36524 | −649.10 | −95.913 | 78.557 | 22.829 |

From the dependence of the logarithm of the Henry-constant $k_0$ on the reciprocal temperature for the gases methane, argon and nitrogen the adsorption heats were calculated. The values of the adsorption heats are in an acceptable range. They are summarized by the example of Norit R1 in Table 6.

From the calculated parameters the excess can be calculated. For all gases a common intersection results in the isotherms, which is represented in Figs. 7–9 for methane, argon and nitrogen on Norit R1.

*Table 12.* Measurements with argon on activated carbon Norit R1 at 298 K.

| $p$ (MPa) | $\rho_{\text{fluid}}$ (g/cm$^3$) | $m^s$ (mg) | $\bar{\Omega}$ (mg/g) | $\bar{\Gamma}_{\text{He}}$ (mg/g) | $\bar{\Gamma}_{3-\text{PIG}}$ (mg/g) |
|---|---|---|---|---|---|
| 0.000 | 0.00000 | 0.00 | m0.00 | 0.000 | 0.000 |
| 0.530 | 0.00857 | 192.06 | 48.52 | 52.472 | 48.271 |
| 1.060 | 0.01720 | 310.64 | 79.05 | 86.985 | 83.653 |
| 1.600 | 0.02604 | 395.19 | 101.28 | 113.302 | 110.930 |
| 2.100 | 0.03428 | 454.10 | 117.13 | 132.954 | 130.655 |
| 2.581 | 0.04223 | 497.59 | 129.15 | 148.648 | 145.913 |
| 3.491 | 0.05741 | 553.70 | 145.51 | 172.016 | 167.747 |
| 4.561 | 0.07542 | 590.59 | 157.66 | 192.474 | 185.291 |
| 5.561 | 0.09240 | 602.94 | 163.61 | 206.263 | 196.413 |
| 6.561 | 0.10949 | 602.13 | 166.36 | 216.905 | 204.003 |
| 7.662 | 0.12840 | 588.71 | 166.34 | 225.613 | 209.392 |
| 8.552 | 0.14377 | 569.80 | 164.37 | 230.730 | 212.031 |
| 9.642 | 0.16265 | 540.17 | 160.37 | 235.450 | 213.632 |
| 10.552 | 0.17844 | 509.98 | 155.70 | 238.073 | 213.860 |
| 11.572 | 0.19615 | 471.67 | 149.38 | 239.922 | 213.138 |
| 13.033 | 0.22146 | 409.21 | 138.45 | 240.678 | 210.645 |
| 14.583 | 0.24820 | 335.95 | 125.12 | 239.693 | 206.502 |
| 16.193 | 0.27571 | 254.92 | 110.03 | 237.301 | 200.926 |
| 17.964 | 0.30553 | 161.59 | 92.32 | 233.357 | 193.636 |
| 20.174 | 0.34191 | 43.19 | 69.60 | 227.432 | 183.256 |
| 22.154 | 0.37353 | −65.58 | 48.43 | 220.852 | 173.111 |
| 24.075 | 0.40316 | −169.75 | 28.03 | 214.128 | 162.769 |
| 26.235 | 0.43515 | −284.69 | 5.40 | 206.271 | 150.808 |
| 28.026 | 0.46054 | −376.92 | −12.80 | 199.784 | 140.813 |
| 30.146 | 0.48925 | −483.70 | −34.00 | 191.844 | 129.062 |
| 32.476 | 0.51913 | −595.50 | −56.22 | 183.412 | 116.456 |
| 35.037 | 0.54998 | −712.89 | −79.64 | 174.231 | 103.199 |
| 38.008 | 0.58333 | −839.41 | −104.87 | 164.401 | 88.839 |
| 40.348 | 0.60788 | −933.61 | −123.70 | 156.899 | 78.418 |
| 43.529 | 0.63903 | −1054.68 | −147.97 | 147.005 | 65.624 |
| 46.599 | 0.66691 | −1161.16 | −169.24 | 138.611 | 54.794 |
| 50.330 | 0.69822 | −1288.21 | −194.95 | 127.355 | 43.586 |

*Table 13.* Measurements with argon on activated carbon Norit R1 at 313 K.

| $p$ (MPa) | $\rho_{\text{fluid}}$ (g/cm$^3$) | $m^s$ (mg) | $\bar{\Omega}$ (mg/g) | $\bar{\Gamma}_{\text{He}}$ (mg/g) | $\bar{\Gamma}_{3-\text{PIG}}$ (mg/g) |
|---|---|---|---|---|---|
| 0.000 | 0.00000 | 0.00 | 0.00 | 0.000 | 0.000 |
| 0.570 | 0.00877 | 165.79 | 42.12 | 46.231 | 41.706 |
| 1.150 | 0.01775 | 270.00 | 69.19 | 77.510 | 73.650 |
| 1.720 | 0.02661 | 342.25 | 88.41 | 100.893 | 97.937 |
| 2.270 | 0.03521 | 394.22 | 102.62 | 119.136 | 116.558 |
| 3.511 | 0.05472 | 470.44 | 124.66 | 150.321 | 146.754 |
| 4.421 | 0.06914 | 502.46 | 134.99 | 167.418 | 161.900 |
| 5.601 | 0.08796 | 521.62 | 142.93 | 184.183 | 175.777 |
| 6.621 | 0.10431 | 523.40 | 146.19 | 195.109 | 184.053 |
| 7.682 | 0.12136 | 514.23 | 146.89 | 203.804 | 189.998 |
| 8.502 | 0.13458 | 501.19 | 145.98 | 209.094 | 193.157 |
| 9.622 | 0.15267 | 476.73 | 143.11 | 214.707 | 195.871 |
| 10.552 | 0.16769 | 451.28 | 139.47 | 218.112 | 196.982 |
| 11.542 | 0.18366 | 420.20 | 134.62 | 220.751 | 197.233 |
| 12.963 | 0.20652 | 369.27 | 126.09 | 222.941 | 196.226 |
| 15.013 | 0.23928 | 286.71 | 111.52 | 223.740 | 192.553 |
| 16.873 | 0.26863 | 204.79 | 96.53 | 222.511 | 187.503 |
| 18.994 | 0.30149 | 105.93 | 77.99 | 219.384 | 180.275 |
| 20.934 | 0.33086 | 12.42 | 60.16 | 215.326 | 172.640 |
| 23.025 | 0.36163 | −88.83 | 40.68 | 210.274 | 163.640 |
| 24.795 | 0.38688 | −174.71 | 24.00 | 205.443 | 155.576 |
| 27.125 | 0.41891 | −286.11 | 2.25 | 198.711 | 144.591 |
| 29.476 | 0.44975 | −395.54 | −19.23 | 191.697 | 133.331 |
| 32.577 | 0.48813 | −534.55 | −46.64 | 182.278 | 118.582 |
| 34.977 | 0.51606 | −636.78 | −66.86 | 175.167 | 107.486 |
| 37.467 | 0.54347 | −738.09 | −86.94 | 167.938 | 96.450 |
| 40.028 | 0.57005 | −837.42 | −106.67 | 160.670 | 85.740 |
| 42.468 | 0.59397 | −926.93 | −124.47 | 154.093 | 76.216 |
| 45.579 | 0.62261 | −1034.74 | −145.93 | 146.067 | 65.127 |
| 47.920 | 0.64290 | −1110.62 | −161.01 | 140.504 | 57.581 |
| 50.240 | 0.66204 | −1182.74 | −175.36 | 135.123 | 50.772 |

The significance and the position of this intersection is to be explained in connection with the characteristics of the respective gas (compressibility) and with the values of the absolute adsorption. This aspect is discussed in the following publication.

### *Gibbs Surface Excess*

According to the Gibbssian thermodynamics the Gibbs excess amount adsorbed $\bar{\Gamma}_{\text{He}}$ was also calculated using the so called helium volume of porous solids $\bar{V}_{\text{ads,He}}$. The resulting values are summerized in the Tables 7–19.

## The Bender Equation

A special thermodynamic equation of state introduced by Bender (Sievers and Schulz, 1981) mentions pressure $p$ for pure substances as a function of temperature $T$ and molar density $\rho_m$ of the fluid. The equation

*Table 14.* Measurements with argon on activated carbon Norit R1 at 328 K.

| $p$ (MPa) | $\rho_{\text{fluid}}$ (g/cm$^3$) | $m^s$ (mg) | $\bar{\Omega}$ (mg/g) | $\bar{\Gamma}_{\text{He}}$ (mg/g) | $\bar{\Gamma}_{3-\text{PIG}}$ (mg/g) |
|---|---|---|---|---|---|
| 0.000 | 0.00000 | 0.00 | 0.00 | 0.000 | 0.000 |
| 0.590 | 0.00866 | 119.22 | 30.69 | 34.791 | 33.107 |
| 1.210 | 0.01780 | 212.20 | 55.04 | 63.467 | 60.594 |
| 1.820 | 0.02683 | 279.61 | 73.11 | 85.809 | 82.269 |
| 2.420 | 0.03574 | 329.53 | 86.87 | 103.793 | 99.661 |
| 3.421 | 0.05067 | 387.13 | 103.56 | 127.540 | 122.242 |
| 4.481 | 0.06656 | 423.98 | 115.33 | 146.834 | 139.853 |
| 5.541 | 0.08253 | 443.22 | 122.79 | 161.857 | 152.846 |
| 6.661 | 0.09944 | 449.15 | 127.17 | 174.238 | 162.918 |
| 6.591 | 0.09838 | 450.12 | 127.22 | 173.791 | 162.379 |
| 7.522 | 0.11246 | 446.75 | 128.82 | 182.058 | 168.703 |
| 8.492 | 0.12715 | 436.36 | 128.82 | 189.005 | 173.624 |
| 9.852 | 0.14775 | 412.78 | 126.60 | 196.539 | 178.249 |
| 11.502 | 0.17269 | 372.30 | 120.99 | 202.734 | 181.110 |
| 12.963 | 0.19468 | 328.51 | 114.06 | 206.212 | 181.740 |
| 14.603 | 0.21919 | 273.16 | 104.74 | 208.495 | 180.793 |
| 16.243 | 0.24347 | 212.10 | 93.98 | 209.221 | 178.479 |
| 17.984 | 0.26888 | 142.54 | 81.33 | 208.601 | 174.854 |
| 20.074 | 0.29882 | 55.28 | 65.13 | 206.576 | 169.268 |
| 22.034 | 0.32626 | −28.78 | 49.28 | 203.713 | 163.109 |
| 24.155 | 0.35512 | −121.24 | 31.61 | 199.712 | 155.710 |
| 26.505 | 0.38600 | −222.82 | 12.07 | 194.784 | 146.882 |
| 28.076 | 0.40596 | −290.37 | −1.03 | 191.133 | 140.745 |
| 29.946 | 0.42899 | −370.02 | −16.56 | 186.507 | 133.292 |
| 32.787 | 0.46242 | −487.27 | −39.50 | 179.389 | 121.873 |
| 35.457 | 0.49216 | −593.13 | −60.29 | 172.670 | 111.243 |
| 37.768 | 0.51658 | −681.01 | −77.60 | 166.928 | 102.272 |
| 40.168 | 0.54074 | −768.68 | −94.90 | 161.062 | 93.280 |
| 43.419 | 0.57157 | −881.42 | −117.19 | 153.368 | 81.773 |
| 46.059 | 0.59512 | −968.17 | −134.37 | 147.337 | 73.076 |
| 50.450 | 0.63160 | −1102.94 | −161.07 | 137.897 | 60.020 |

has the form of a virial equation stopped after the sixth power. It possesses also an exponential function as correction term:

$$p = RT\rho_m + B\rho_m^2 + C\rho_m^3 + D\rho_m^4 + E\rho_m^5 + F\rho_m^6 + \left(G + H\rho_m^2\right)\rho_m^3 \exp\left(-a_{20}\rho_m^2\right)$$

$R$ is the universal gas constant, $B, C, D, E, F, G$ and $H$ are temperature dependent coefficients of the equation of state, $a_{20}$ is a non-linear parameter.

*Table 15.* Measurements with argon on activated carbon Norit R1 at 343 K.

| $p$ (MPa) | $\rho_{\text{fluid}}$ (g/cm$^3$) | $m^s$ (mg) | $\bar{\Omega}$ (mg/g) | $\bar{\Gamma}_{\text{He}}$ (mg/g) | $\bar{\Gamma}_{3-\text{PIG}}$ (mg/g) |
|---|---|---|---|---|---|
| 0.000 | 0.00000 | 0.00 | 0.00 | 0.000 | 0.000 |
| 0.610 | 0.00856 | 99.40 | 25.45 | 29.539 | 27.790 |
| 1.210 | 0.01700 | 171.80 | 44.37 | 52.487 | 50.085 |
| 1.780 | 0.02505 | 226.30 | 58.89 | 70.855 | 67.697 |
| 2.581 | 0.03637 | 283.40 | 74.60 | 91.976 | 87.899 |
| 3.571 | 0.05043 | 331.50 | 88.61 | 112.696 | 107.389 |
| 4.461 | 0.06311 | 359.70 | 97.57 | 127.717 | 121.034 |
| 5.621 | 0.07967 | 379.20 | 105.10 | 143.153 | 134.733 |
| 6.541 | 0.09282 | 385.70 | 108.90 | 153.244 | 143.079 |
| 7.552 | 0.10727 | 384.70 | 111.12 | 162.364 | 150.247 |
| 8.692 | 0.12358 | 375.50 | 111.67 | 170.707 | 156.342 |
| 9.462 | 0.13458 | 365.10 | 111.04 | 175.324 | 159.481 |
| 10.422 | 0.14827 | 348.70 | 109.41 | 180.233 | 162.471 |
| 11.242 | 0.15994 | 331.40 | 107.22 | 183.618 | 164.337 |
| 12.813 | 0.18220 | 292.40 | 101.59 | 188.627 | 166.443 |
| 14.543 | 0.20653 | 241.90 | 93.54 | 192.199 | 166.951 |
| 16.263 | 0.23047 | 185.50 | 84.00 | 194.089 | 165.990 |
| 18.074 | 0.25531 | 121.90 | 72.87 | 194.830 | 163.744 |
| 20.094 | 0.28253 | 46.60 | 59.33 | 194.290 | 160.066 |
| 22.114 | 0.30917 | −31.40 | 45.03 | 192.718 | 155.440 |
| 26.415 | 0.36356 | −201.10 | 13.32 | 186.991 | 143.393 |
| 27.996 | 0.38269 | −263.70 | 1.46 | 184.267 | 138.459 |
| 30.096 | 0.40734 | −346.30 | −14.28 | 180.302 | 131.644 |
| 32.607 | 0.43565 | −442.50 | −32.68 | 175.421 | 123.263 |
| 34.977 | 0.46122 | −531.10 | −49.72 | 170.597 | 115.258 |
| 37.417 | 0.48638 | −619.30 | −66.73 | 165.605 | 107.051 |
| 40.048 | 0.51221 | −711.00 | −84.47 | 160.203 | 98.365 |
| 43.389 | 0.54318 | −822.50 | −106.12 | 153.353 | 87.735 |
| 46.559 | 0.57078 | −922.70 | −125.61 | 147.042 | 78.191 |
| 50.230 | 0.60073 | −1032.10 | −146.92 | 140.037 | 67.934 |

*Table 16.* Measurements with methane on activated carbon Norit R1 at 298 K.

| $p$ (MPa) | $\rho_{\text{fluid}}$ (g/cm$^3$) | $m^s$ (mg) | $\bar{\Omega}$ (mg/g) | $\bar{\Gamma}_{\text{He}}$ (mg/g) | $\bar{\Gamma}_{3-\text{PIG}}$ (mg/g) |
|---|---|---|---|---|---|
| 0.00 | 0.00000 | 0.000 | 0.000 | 0.000 | 0.000 |
| 0.32 | 0.00208 | 152.680 | 35.863 | 36.825 | 34.750 |
| 0.74 | 0.00485 | 232.690 | 55.416 | 57.656 | 58.363 |
| 1.82 | 0.01216 | 315.380 | 77.637 | 83.250 | 83.408 |
| 3.20 | 0.02190 | 340.180 | 87.719 | 97.829 | 93.999 |
| 4.69 | 0.03294 | 329.720 | 90.321 | 105.525 | 97.489 |

(*Continued on next page.*)

*Table 16.* (*Continued*).

| $p$ (MPa) | $\rho_{\text{fluid}}$ (g/cm$^3$) | $m^s$ (mg) | $\bar{\Omega}$ (mg/g) | $\bar{\Gamma}_{\text{He}}$ (mg/g) | $\bar{\Gamma}_{3-\text{PIG}}$ (mg/g) |
|---|---|---|---|---|---|
| 6.07 | 0.04362 | 301.140 | 88.620 | 108.756 | 97.630 |
| 7.99 | 0.05916 | 242.980 | 82.349 | 109.657 | 95.165 |
| 10.19 | 0.07770 | 158.810 | 71.489 | 107.355 | 89.910 |
| 12.02 | 0.09343 | 80.450 | 60.687 | 103.815 | 84.137 |
| 13.92 | 0.10971 | −6.150 | 48.247 | 98.889 | 77.153 |
| 16.05 | 0.12745 | −103.270 | 34.064 | 92.896 | 68.516 |
| 18.13 | 0.14382 | −193.600 | 20.812 | 87.201 | 59.675 |
| 20.08 | 0.15804 | −273.030 | 9.082 | 82.036 | 51.405 |
| 21.86 | 0.16998 | −340.590 | −0.966 | 77.498 | 44.151 |
| 24.00 | 0.18301 | −414.870 | −12.058 | 72.422 | 36.083 |
| 25.85 | 0.19318 | −473.210 | −20.799 | 68.375 | 29.852 |
| 27.98 | 0.20376 | −533.970 | −29.908 | 64.149 | 23.632 |
| 30.05 | 0.21302 | −587.500 | −37.959 | 60.375 | 18.578 |
| 32.62 | 0.22334 | −647.350 | −46.980 | 56.115 | 13.568 |
| 34.98 | 0.23183 | −696.890 | −54.466 | 52.549 | 10.045 |
| 37.51 | 0.24007 | −743.770 | −61.461 | 49.357 | 7.204 |
| 40.11 | 0.24775 | −787.400 | −67.964 | 46.398 | 5.076 |
| 43.46 | 0.25667 | −838.290 | −75.567 | 42.913 | 3.203 |
| 46.69 | 0.26441 | −882.160 | −82.096 | 39.958 | 2.039 |
| 49.45 | 0.27047 | −916.170 | −87.132 | 37.720 | 1.381 |

*Table 17.* Measurements with methane on activated carbon Norit R1 at 313 K.

| $p$ (MPa) | $\rho_{\text{fluid}}$ (g/cm$^3$) | $m^s$ (mg) | $\bar{\Omega}$ (mg/g) | $\bar{\Gamma}_{\text{He}}$ (mg/g) | $\bar{\Gamma}_{3-\text{PIG}}$ (mg/g) |
|---|---|---|---|---|---|
| 0.00 | 0.00000 | 0.000 | 0.000 | 0.000 | 0.000 |
| 0.33 | 0.00204 | 115.790 | 27.408 | 28.366 | 26.617 |
| 0.92 | 0.00574 | 205.470 | 49.595 | 52.289 | 52.816 |
| 1.66 | 0.01048 | 260.660 | 64.360 | 69.274 | 69.576 |
| 3.02 | 0.01944 | 297.620 | 76.868 | 85.983 | 83.498 |
| 4.41 | 0.02894 | 298.140 | 81.287 | 94.857 | 89.067 |
| 5.98 | 0.04006 | 276.620 | 81.401 | 100.190 | 90.950 |
| 7.63 | 0.05216 | 237.890 | 78.017 | 102.478 | 90.292 |
| 10.11 | 0.07091 | 160.170 | 68.729 | 101.986 | 86.360 |
| 11.92 | 0.08483 | 95.020 | 60.125 | 99.908 | 82.022 |
| 14.02 | 0.10092 | 14.530 | 48.999 | 96.329 | 75.926 |
| 16.13 | 0.11673 | −67.890 | 37.304 | 92.048 | 69.010 |
| 17.96 | 0.12991 | −138.660 | 27.085 | 88.012 | 62.629 |
| 20.01 | 0.14390 | −216.370 | 15.642 | 83.130 | 55.327 |
| 21.94 | 0.15620 | −284.720 | 5.575 | 78.830 | 48.534 |
| 24.12 | 0.16901 | −356.250 | −4.988 | 74.274 | 41.201 |
| 26.02 | 0.17925 | −413.900 | −13.540 | 70.524 | 35.266 |
| 28.11 | 0.18957 | −471.610 | −22.068 | 66.837 | 29.349 |
| 29.90 | 0.19769 | −517.360 | −28.856 | 63.858 | 24.841 |
| 32.23 | 0.20737 | −572.030 | −36.978 | 60.275 | 19.766 |
| 34.62 | 0.21638 | −623.420 | −44.655 | 56.825 | 15.454 |
| 37.52 | 0.22624 | −679.500 | −53.018 | 53.086 | 11.316 |
| 40.06 | 0.23406 | −723.830 | −59.619 | 50.151 | 8.532 |
| 43.36 | 0.24326 | −776.240 | −67.443 | 46.641 | 5.850 |
| 46.87 | 0.25205 | −826.160 | −74.881 | 43.327 | 3.878 |
| 50.17 | 0.25955 | −868.620 | −81.200 | 40.523 | 2.616 |

*Table 18.* Measurements with methane on activated carbon Norit R1 at 328 K.

| $p$ (MPa) | $\rho_{\text{fluid}}$ (g/cm$^3$) | $m^s$ (mg) | $\bar{\Omega}$ (mg/g) | $\bar{\Gamma}_{\text{He}}$ (mg/g) | $\bar{\Gamma}_{3-\text{PIG}}$ (mg/g) |
|---|---|---|---|---|---|
| 0.00 | 0.00000 | 0.00 | 0.000 | 0.000 | 0.000 |
| 0.42 | 0.00248 | 112.11 | 26.765 | 27.940 | 26.174 |
| 0.93 | 0.00553 | 174.49 | 42.412 | 45.030 | 45.050 |
| 1.64 | 0.00984 | 224.46 | 55.790 | 60.445 | 60.368 |
| 3.09 | 0.01885 | 264.94 | 69.127 | 78.049 | 75.384 |
| 4.47 | 0.02769 | 268.33 | 73.905 | 87.013 | 81.446 |
| 6.37 | 0.04025 | 244.71 | 74.187 | 93.239 | 84.402 |
| 7.49 | 0.04783 | 221.81 | 72.380 | 95.022 | 84.560 |
| 8.96 | 0.05794 | 185.09 | 68.556 | 95.981 | 83.654 |
| 10.78 | 0.07061 | 132.20 | 62.194 | 95.616 | 81.292 |
| 12.34 | 0.08151 | 82.24 | 55.702 | 94.286 | 78.470 |
| 14.02 | 0.09319 | 25.44 | 47.997 | 92.110 | 74.809 |
| 15.98 | 0.10659 | −42.43 | 38.537 | 88.991 | 69.925 |
| 17.93 | 0.11951 | −109.82 | 28.972 | 85.544 | 64.601 |
| 20.19 | 0.13380 | −185.75 | 18.074 | 81.411 | 58.086 |
| 22.00 | 0.14462 | −243.87 | 9.677 | 78.135 | 52.764 |
| 23.91 | 0.15538 | −302.49 | 1.137 | 74.685 | 47.191 |
| 25.79 | 0.16528 | −356.98 | −6.843 | 71.393 | 41.867 |
| 27.79 | 0.17509 | −410.82 | −14.719 | 68.159 | 36.488 |
| 29.73 | 0.18391 | −459.89 | −21.948 | 65.108 | 31.636 |
| 32.39 | 0.19500 | −522.14 | −31.167 | 61.137 | 25.661 |
| 35.70 | 0.20735 | −591.21 | −41.377 | 56.771 | 19.399 |
| 38.26 | 0.21594 | −639.28 | −48.483 | 53.733 | 15.431 |
| 40.09 | 0.22164 | −671.25 | −53.216 | 51.698 | 13.028 |
| 43.46 | 0.23129 | −725.44 | −61.241 | 48.241 | 9.441 |
| 46.80 | 0.23993 | −774.12 | −68.465 | 45.107 | 6.788 |
| 50.52 | 0.24865 | −822.92 | −75.681 | 42.017 | 4.655 |

*Table 19.* Measurements with methane on activated carbon Norit R1 at 343 K.

| $p$ (MPa) | $\rho_{\text{fluid}}$ (g/cm$^3$) | $m^{\text{s}}$ (mg) | $\bar{\Omega}$ (mg/g) | $\bar{\Gamma}_{\text{He}}$ (mg/g) | $\bar{\Gamma}_{3-\text{PIG}}$ (mg/g) |
|---|---|---|---|---|---|
| 0.00 | 0.00000 | 0.000 | 0.000 | 0.000 | 0.000 |
| 0.43 | 0.00243 | 93.400 | 22.461 | 23.621 | 21.806 |
| 0.90 | 0.00511 | 148.020 | 36.166 | 38.606 | 37.384 |
| 1.52 | 0.00868 | 189.210 | 47.203 | 51.349 | 50.812 |
| 3.14 | 0.01821 | 233.490 | 61.644 | 70.341 | 68.654 |
| 4.94 | 0.02911 | 236.030 | 67.159 | 81.063 | 76.653 |
| 6.04 | 0.03591 | 225.570 | 67.846 | 85.001 | 78.870 |
| 8.07 | 0.04870 | 191.230 | 65.780 | 89.044 | 80.156 |
| 10.03 | 0.06124 | 146.260 | 61.169 | 90.421 | 79.282 |
| 12.26 | 0.07557 | 86.420 | 53.970 | 90.069 | 76.712 |
| 14.04 | 0.08694 | 33.310 | 46.969 | 88.502 | 73.824 |
| 15.98 | 0.09915 | −25.840 | 38.963 | 86.323 | 70.063 |
| 18.05 | 0.11181 | −89.980 | 30.025 | 83.436 | 65.534 |
| 20.14 | 0.12411 | −153.690 | 21.021 | 80.308 | 60.592 |
| 21.96 | 0.13435 | −207.540 | 13.338 | 77.516 | 56.110 |
| 24.03 | 0.14540 | −266.380 | 4.883 | 74.340 | 50.933 |
| 26.20 | 0.15628 | −325.220 | −3.652 | 71.001 | 45.545 |
| 28.25 | 0.16589 | −377.520 | −11.267 | 67.974 | 40.601 |
| 30.38 | 0.17520 | −428.590 | −18.734 | 64.955 | 35.708 |
| 32.59 | 0.18417 | −477.950 | −25.960 | 62.016 | 30.970 |
| 34.87 | 0.19276 | −524.930 | −32.820 | 59.259 | 26.502 |
| 37.43 | 0.20166 | −574.930 | −40.229 | 56.100 | 22.032 |
| 40.67 | 0.21192 | −632.360 | −48.719 | 52.512 | 17.212 |
| 43.22 | 0.21931 | −673.510 | −54.786 | 49.974 | 14.048 |
| 46.67 | 0.22848 | −724.410 | −62.280 | 46.860 | 10.561 |
| 50.24 | 0.23710 | −772.340 | −69.341 | 43.916 | 7.780 |

## Conclusion

In the course of this project thermodynamically consistent sets of data of adsorption equilibria were measured and analyzed highly precisely by the use of a magnetic suspension balance at pressures of up to 50 MPa. Gravimetric measurements of adsorption with the pure gases methane, argon and nitrogen were carried out at 298, 313, 328 and 343 K on two different adsorbents. The activated carbons were characterized with regard to their volume of pores and their internal surface.

The description of the excess by means of the original three-parameter isothermal equation, which was applied in the pressure range of up to 15 MPa is not possible due to the "unknown" or inaccurate volume of the adsorbent. Therefore, it was proposed to use the precisely measured values of adsorption directly for the thermodynamic modelling without additional information (volume of the adsorbents). The excess is determined thereby subsequently from the parameters of the extended three-parameter isothermal equation.

## Notation

| | |
|---|---|
| $p$ | Pressure (MPa) |
| $\bar{\Gamma}_{\text{He}}$ | Excess adsorption with buoyancy correction (mg/g) |
| $\bar{\Gamma}_{3-\text{PIG}}$ | Excess adsorption calculated from 3-PIG (mg/g) |
| $I_0$ | Maximal loading (mg/g) |
| $k_0$ | Henry-constant (MPa) |
| $v_0$ | Molar volume (cm$^3$/mol) |
| $f$ | Fugacity (MPa) |
| $R$ | Gas constant (cm$^3 *$ MPa/mol $*$ K) |
| $T$ | Temperature (K) |
| $m^{\text{s}}$ | Microbalance signal (mg) |
| $m$ | Mass of adsorbent (g) |
| $\bar{\Omega}$ | Specific mass of the sample of adsorbent at the micro-balance (mg/g) |
| $\rho_{\text{fluid}}$ | Density of the fluid (g/cm$^3$) |
| $\rho_{\text{He}}$ | Density of Helium (g/cm$^3$) |
| $V_{\text{ads}}$ | Volume of the adsorbent (cm$^3$) |
| $\bar{V}_{\text{ads}}$ | Specific volume of the adsorbent (cm$^3$/g) |
| $V_{\text{cont}}$ | Volume of container (cm$^3$) |

## Acknowledgment

Financial support of this project by the Deutsche Forschungsgemeinschaft (Project IIC1-Ha 1 1951/8-1) is gratefully acknowledged. Discussion with Alan Myers are as well gratefully acknowledged.

## References

Harting, P., J. Germanus, and S. Beutekamp, *Fortschrittberichte VDI, Reihe 3 Verfahrenstechnik*, **554**, 147–161.

Malbrunot, P., D. Vidal, J. Vermesse, R. Chahine, and T.K. Bose, "Adsorption Measurements of Argon, Neon, Krypton, Nitrogen and Methane on Activated Carbon up to 650 MPa," *Langmuir*, **8**, 577–580 (1992).

Malbrunot, P., D. Vidal, J. Vermesse, R. Chahine, and T.K. Bose, "Adsorbent Helium Density Measurement and Its Effect on Adsorption Isotherms at High Pressure," *Langmuir*, **13**, 539–544 (1997).

Neimark, A.V. and P.I. Ravikovich, "Calibration of Pore Volume in Adsorption Experiments and Theoretical Models," *Langmuir*, **13**, 5148–5160 (1997).

Platzer, B. and G. Maurer, "Application of a Generalized Bender Equation of State to the Description of Vapour-Liquid Equilibria in Binary Systems," *Fluid Phase Equlibria*, **84**, 79–110 (1993).

Salem, M., "Thermodynamik der Hochdruckadsorption einfacher Gase an porösen Adsorbenzien," Dissertation, University of Leipzig, 1997.

Sievers, U. and S. Schulz, *VDI-Forschungsheft*, **609**, 45–52 (1981).

Sircar, S., "On the Measurements of Gibbsian Surface Excess," Air Products and Chemicals, Inc. (1999).

Staudt, R., S. Bohn, F. Dreisbach, and J.U. Keller, "Gravimetric and Volumetric Measurements of Helium Adsorption Equilibria on Different Porous Solids," *Characterisation of Porous Solids*, **IV**, 261–266.

Staudt, R., G. Saller, M. Tomalla, and J.U. Keller, "A Note on Gravimetric Measurements of Gas-Adsorption Equilibria," *Ber. Bunsenges. Phys. Chem. Bd.*, **97**(1), 98–105 (1993).

Talu, O., "Needs, Status, Techniques and Problems with Binary Gas Adsorption Experiments," *Adv. Colloid Interface Sci.*, **76/77**, 227–269 (1998).

Vazquez, I., M.P. Russell, D.R. Smith, and R. Radebaugh, "Helium Adsorption on Activated Carbons at Temperatures Between 4 and 76 K," *Advances in Cryogenic Engineering*, **33**, 1013–1021 (1987).